

# Dynamic Range Optimisation of CMOS Image Sensors dedicated to Space Applications

P. MARTIN-GONTHIER\*, P.MAGNAN\*\*, F. CORBIERE\*\*\*, Magali ESTRIBEAU,  
Nicolas HUGER, Luc BOUCHER

SUPAERO – Integrated Image Sensors Laboratory  
10 avenue Edouard Belin, 31400 Toulouse, France

## ABSTRACT

Nowadays, CMOS image sensors are widely considered for space applications. Their performances have been significantly enhanced with the use of CIS (CMOS Image Sensor) processes in term of dark current, quantum efficiency and conversion gain. Dynamic Range (DR) remains an important parameter for a lot of applications. Most of the dynamic range limitation of CMOS image sensors comes from the pixel. During work performed in collaboration with EADS Astrium, SUPAERO/CIMI laboratory has studied different ways to improve dynamic range and test structures have been developed to perform analysis and characterisation. A first way to improve dynamic range will be described, consisting in improving the voltage swing at the pixel output. Test vehicles and process modifications made to improve voltage swing will be depicted. We have demonstrated a voltage swing improvement more than 30%. A second way to improve dynamic range is to reduce readout noise. A new readout architecture has been developed to perform a correlated double sampling readout. Strong readout noise reduction will be demonstrated by measurements performed on our test vehicle. A third way to improve dynamic range is to control conversion gain value. Indeed, in 3 TMO pixel structure, dynamic range is related to conversion gain through reset noise which is dependant of photodiode capacitance. Decrease and increase of conversion gain have been performed with different design techniques. A good control of the conversion gain will be demonstrated with variation in the range of 0.05 to 3 of initial conversion gain.

**Keywords:** APS, CMOS Image Sensor, dynamic range, readout techniques, conversion gain

## 1. INTRODUCTION

CMOS image sensors are nowadays extensively considered for several space applications. CMOS standard processes, which are developed for digital and mixed signal applications, are really attractive particularly because of their low power consumption, applicability for on-chip signal processing and large availability. However, electro-optic performances are often inadequate for high end applications. Several ways have been explored to improve image sensor performances to a very high level [1] [2] [3].

Dynamic Range (DR), defined as  $\frac{\text{Maximum\_usable\_output\_linear\_voltage\_swing}}{\text{noise\_in\_dark}}$  remains an important

parameter for a lot of applications. Most of the dynamic range limitation of CMOS image sensors comes from the pixel itself. During programs performed in collaboration with EADS Astrium, SUPAERO/CIMI laboratory has studied different ways to improve it and test structures have been developed in order to perform analysis and characterisation.

Section 2 defines the dynamic range equation for a CMOS image sensor for a common readout circuit composed of two stages. This equation highlights parameters which impact strongly the dynamic range.

Section 3 presents the first way to improve the dynamic range. It consists in increasing the voltage swing at the output of the pixel. In collaboration with the foundry, process modifications were made to optimize implant settings in order to enhance threshold voltage and reducing body effect of MOS transistors in the pixel. Test vehicle and process modifications are depicted.

\* philippe.martin\_gonthier@supaero.fr; phone +33 5 62 17 83 69; fax +33 5 62 17 83 45

\*\* pierre.magnan@supaero.fr; phone +33 5 62 17 80 79; fax +33 5 62 17 83 45

\*\*\* franck.corbriere@supaero.fr; phone +33 5 62 17 82 96; fax +33 5 62 17 83 45

In section 4, a new architecture allowing to improve the dynamic range is depicted. This architecture reduces readout noise. In the common photodiode pixel, so called 3T pixel with 3 MOS transistors in-pixel, noise from reset phase generally dominates other noise sources ( $\sqrt{\frac{kT}{C_{PH}}}$  for hard reset or close to  $\sqrt{\frac{kT}{2.C_{PH}}}$  for soft reset with  $C_{PH}$  : photodiode capacitance). This readout architecture has been developed to perform a correlated double sampling readout. Details are given and strong readout noise reduction is demonstrated by measurements performed on our test vehicle. Section 5 presents a third way to improve the dynamic range. This technique consists in controlling the conversion gain value for different pixel. Indeed, in 3 T MOS pixel structure, dynamic range is related to conversion gain through reset noise which is dependant of photodiode capacitance. Decrease and increase of conversion gain for a given pixel pitch (13 $\mu$ m) have been performed with different design techniques. A control of the conversion gain will be demonstrated with variation in the range of 0.05 to 3 of initial conversion gain. In conclusion of the paper, a review of improvements obtained on voltage swing, conversion gain and noise level is made to understand impact on dynamic range. All the test vehicles presented in this paper were designed by CIMI and co-funded by CIMI and EADS-Astrium.

## 2. DYNAMIC RANGE DEFINITION FOR CMOS IMAGE SENSORS

In this section, a definition of the dynamic range for CMOS image sensors is explicated. For a system as depicted in Figure 1, the output dynamic range of a CMOS image sensor is defined by :

$$DR = \frac{\text{Maximum\_usable\_output\_linear\_voltage\_swing}}{\text{noise\_in\_dark}}$$

$$\hookrightarrow \text{Maximum\_usable\_output\_linear\_voltage\_swing} = A_{TOT}V_{MAX} - A_{TOT}V_{DARK}$$

$$\hookrightarrow \text{Noise\_in\_dark} = \sqrt{A_{TOT}^2 V_{NOISE\_DARK}^2 + 2A_{TOT}^2 V_{RESET}^2 + V_{READOUT\_NOISE}^2}$$

With :  $V_{MAX}$  = Maximum linear voltage on the photodiode (or readout node)  
 $V_{DARK}$  = Voltage due to dark current  
 $V_{NOISE\_DARK}$  = Noise voltage due to dark current  
 $V_{RESET}$  = Noise voltage due to reset phase  
 $V_{READOUT\_NOISE}$  = Noise voltage due to readout circuit \*  
 $A_{TOT}$  = Readout circuit gain\*  
 \* including pixel column and output stage

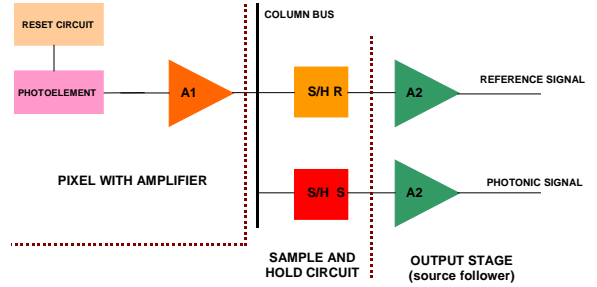


Figure 1 : Photo element and readout circuit synoptic

The readout circuit is generally differential. The reset noise is affected by this differential readout : reset noise is doubled. The  $V_{READOUT\_NOISE}$  takes into account this readout circuit feature.

$$\text{The dynamic range can be expressed by : } DR = \frac{V_{MAX} - V_{DARK}}{\sqrt{V_{NOISE\_DARK}^2 + 2V_{RESET}^2 + \frac{V_{READOUT\_NOISE}^2}{A_{TOT}^2}}}$$

The noise voltage for the reset phase is given by  $V_{RESET}^2 = \frac{kT}{\alpha C_{PH}}$  [4][5][6] and  $G_{C\_PH} = \frac{q}{C_{PH}}$

With  $\alpha$  : coefficient between 1 and 2.  $\alpha \approx 1$  for hard reset mode and  $\alpha \approx 2$  for soft reset mode  
 $G_{C\_PH}$  : Conversion gain on the integration node (or readout node)  
 $C_{PH}$  : Capacitance on the integration node (or readout node)

Using the previous definition of noise voltage for the reset phase, the dynamic range becomes :

$$DR = \frac{V_{MAX} - V_{DARK}}{\sqrt{V_{NOISE\_DARK}^2 + 2\frac{kT}{\alpha q} G_{C\_PH} + \frac{V_{READOUT\_NOISE}^2}{A_{TOT}^2}}} \quad (1)$$

In order to illustrate the previous equation, following figures show the impact of the various parameters on the Dynamic Range. In case of 4T photodiode or 3T photodiode associated with a special readout circuit implementation, the  $\frac{kT}{\alpha q} G_{C\_PH}$  term (reset noise) is cancelled by the Correlated Double Sampling (CDS) mode [7].

Figure 2 shows variations of dynamic range versus pixel pitch in case of “hard reset” mode, “soft reset” mode and CDS mode for the CIS 0.35 $\mu$ m process considered. Other parameters are fixed :  $V_{MAX}=1V$ ,  $T_{INT}=10ms$ ,  $V_{READOUT\_NOISE}=150\mu V$ ,  $A_{TOT}=0.6$ ,  $J_{DARK}=200pA/cm^2$  (dark current density). Active part in the pixel stays constant so fill factor decrease with pixel pitch. These curves show that for both “hard” and “soft” reset modes, the dynamic range is increasing with pixel pitch. This increase is due to reset noise dependence on pixel pitch. The dynamic range stays constant for CDS mode except for small pixel where conversion gain becomes very high and thus dark current noise impact is higher.

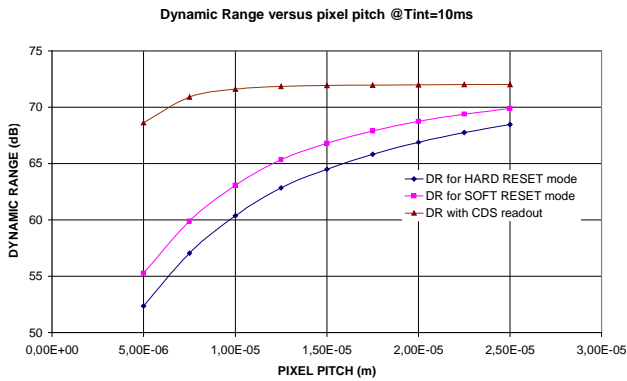


Figure 2 : Dynamic Range versus pixel pitch @  $V_{MAX}=1V$ ,  $T_{INT}=10ms$ ,  $V_{READOUT\_NOISE}=150\mu V$ ,  $A_{TOT}=0.6$ ,  $J_{DARK}=200pA/cm^2$

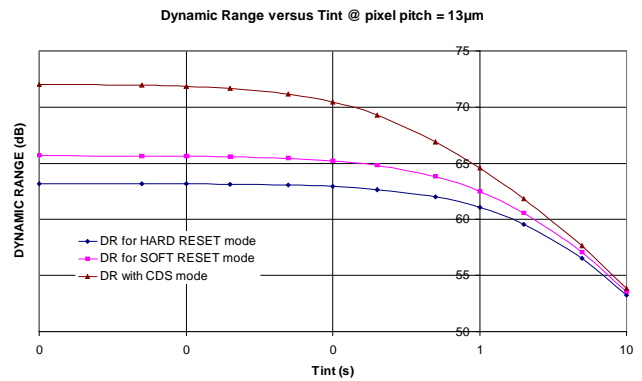


Figure 3 : Dynamic Range versus  $T_{INT}$  @  $V_{MAX}=1V$ , pixel pitch=13 $\mu$ m,  $V_{READOUT\_NOISE}=150\mu V$ ,  $A_{TOT}=0.6$ ,  $J_{DARK}=200pA/cm^2$

Figure 3 depicts evolution of dynamic range versus integration time. Pixel pitch is fixed to 13 $\mu$ m. For the three modes, curves show a weak impact of integration time on dynamic range. Degradation becomes important when integration time is higher than 100ms. This is due to dark current integration on photodiode, reducing the maximum usable linear voltage swing and the increasing of dark current noise.

Figure 4 illustrates dynamic range behavior versus  $V_{MAX}$  which is the maximum linear voltage swing on photodiode. Pixel pitch is fixed to 13 $\mu$ m and integration time to 10ms. Curves demonstrate an important increase of DR while  $V_{MAX}$  is increasing for the three modes. A dynamic range beyond 70 dB can be reached with a readout circuit allowing Correlated Double Sampling.

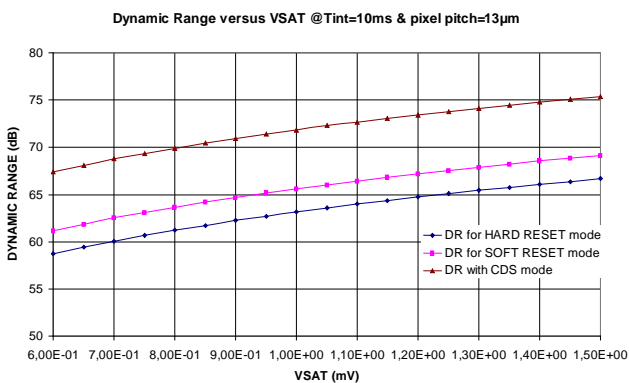


Figure 4 : Dynamic Range versus  $V_{MAX}$  @  $T_{INT}=10ms$ , pixel pitch=13 $\mu$ m,  $V_{READOUT\_NOISE}=150\mu V$ ,  $A_{TOT}=0.6$ ,  $J_{DARK}=200pA/cm^2$

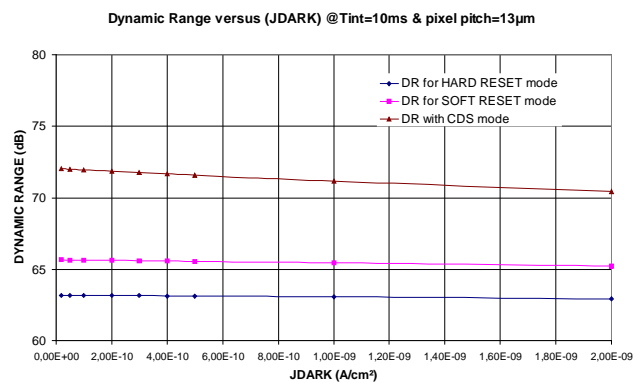


Figure 5 : Dynamic Range versus  $J_{DARK}$  @  $T_{INT}=10ms$ , pixel pitch=13 $\mu$ m,  $V_{READOUT\_NOISE}=150\mu V$ ,  $A_{TOT}=0.6$ ,  $V_{MAX}=1V$

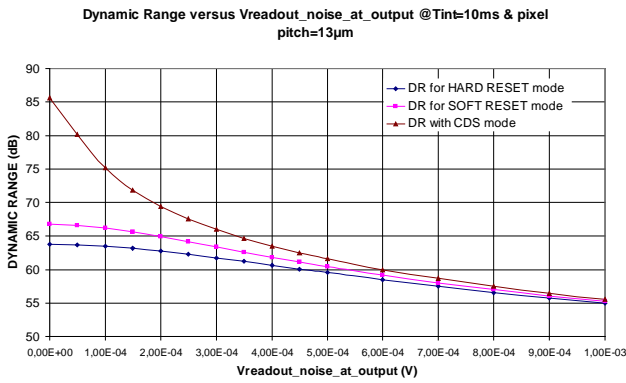


Figure 6 : Dynamic Range versus  $V_{\text{READOUT\_NOISE}}$  with CDS mode @  $T_{\text{INT}}=10\text{ms}$ , pixel pitch= $13\mu\text{m}$ ,  $A_{\text{TOT}}=0.6$ ,  $V_{\text{SAT}}=1\text{V}$ ,  $J_{\text{DARK}}=200\text{pA/cm}^2$

Figure 5 depicts dynamic range versus dark current density with a fixed integration time of 10 ms and a fixed pixel pitch of  $13\mu\text{m}$ . Dark current density have a weak impact on dynamic range for this integration time. DR stays relatively constant for the three mode (“hard”, “soft” and CDS).

Dynamic range dependence on readout circuit noise is depicted in Figure 6, showing a strong impact on the dynamic range in the case of the CDS mode. However, this impact is limited for the both “hard” and “soft” reset modes.

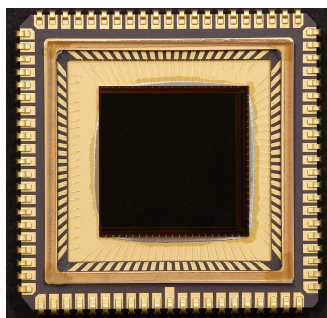
All these curves allow to identify clearly parameters having a major impact on Dynamic Range. These parameters are maximum linear voltage swing on photodiode, reset noise and conversion gain. Next sections of this paper explain optimization work performed by CIMI to enhance dynamic range.

### 3. IMPACT AND OPTIMISATION OF PHOTODIODE VOLTAGE SWING ON DYNAMIC RANGE

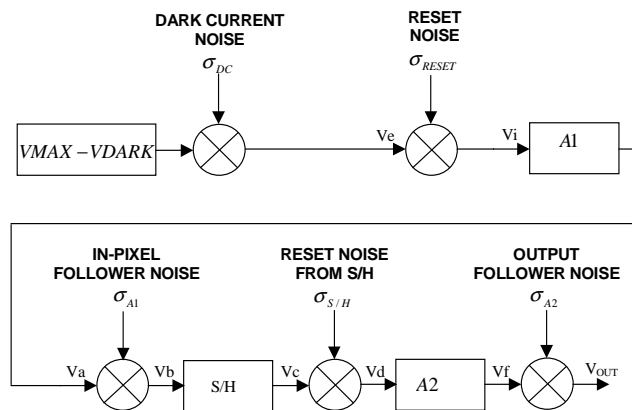
In the previous section, the dynamic range equation has demonstrated the impact of the photodiode voltage swing  $V_{\text{MAX}}$  on the dynamic range. In order to increase dynamic range of a CMOS image sensor, the photodiode voltage swing must be increased. CIMI laboratory has designed, in collaboration with the UMC foundry, a test vehicle allowing to enhance the photodiode voltage swing without degradation of photodiode dark current. The process, coming from UMC, is  $0.35\mu\text{m}$  CIS (CMOS Image Sensor) dedicated to detection applications. This process is optimized for quantum efficiency, charge collection and low dark current thanks to special photodiode doping profile.

The test vehicle, named COBRA1M, is a  $1\text{K}\times 1\text{K}$  common (3T) photodiode array. The pixel pitch is  $13\mu\text{m}$ . Readout circuit architecture is the same as depicted in Figure 1. A photography of COBRA1M is depicted on Figure 7a).

The readout circuit is composed of two amplification stages and a sample and hold circuit to perform sampling on reference signal and photonic signal. The two amplification stages are based on source follower structures.



a) Photography



b) Noise equivalent model for a CMOS image sensor in dark

Figure 7 : Photography and noise equivalent model of COBRA1M

The noise equivalent model associated to this readout circuit is shown in Figure 7 b). The output dynamic range for this CMOS image sensor, when taking into account the readout architecture is defined by :

$$DR = \frac{\text{Maximum\_usable\_output\_linear\_voltage\_swing}}{\text{noise\_in\_dark}}$$

$$\text{Maximum\_usable\_output\_linear\_voltage\_swing} = A_1 A_2 (V_{MAX} - V_{DARK})$$

$$\text{Noise\_in\_dark} = \sqrt{A_1^2 A_2^2 \sigma_{NOISE\_DARK}^2 + 2A_1^2 A_2^2 \sigma_{RESET}^2 + 2A_2^2 \sigma_{A1}^2 + 2A_2^2 \sigma_{SH}^2 + 2\sigma_{A2}^2}$$

With :  $V_{MAX}$  = Maximum linear voltage on the photodiode (or readout node)  
 $V_{DARK}$  = Voltage due to dark current  
 $\sigma_{NOISE\_DARK}$  = Noise voltage due to dark current  
 $\sigma_{RESET}$  = Noise voltage due to reset phase  
 $\sigma_{A1}$  = Noise voltage due to first stage amplifier  
 $\sigma_{A2}$  = Noise voltage due to second stage amplifier  
 $\sigma_{SH}$  = Noise voltage due to S/H phase  
 $A_1$  = First stage gain  
 $A_2$  = Second stage gain

The dynamic range can be expressed by :

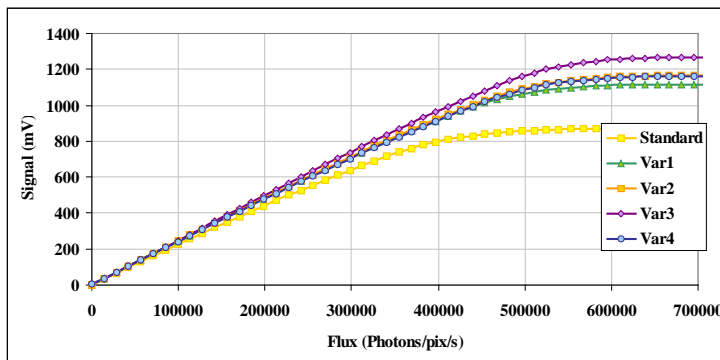
$$DR = \frac{(V_{MAX} - V_{DARK})}{\sqrt{\sigma_{NOISE\_DARK}^2 + 2 \frac{kT}{\alpha q} G_{C\_PH} + 2 \frac{\sigma_{A1}^2}{A_1^2} + 2 \frac{\sigma_{SH}^2}{A_1^2} + 2 \frac{\sigma_{A2}^2}{A_1^2 A_2^2}}}$$

With the assumption about reset noise predominance compared to the other noise for this kind of pixel, the dynamic range can be expressed by :

$$DR \approx \frac{(V_{MAX} - V_{DARK})}{\sqrt{2 \frac{kT}{\alpha q} G_{C\_PH}}}$$

The readout circuit for this vehicle is common as depicted on Figure 7 b). The 3T pixel is composed of a reset transistor, a source follower transistor and the row selection transistor. These 3 in-pixel transistors are impacted by special doping implant. Features as threshold voltage and leakage current of the reset and the source follower transistor are very important. If threshold voltage of source follower decreases the photodiode output voltage increases. A special care must be taken to keep a low leakage current in order to avoid dark current.

Four variations of photodiode doping implant were implemented to decrease threshold voltage without changing leakage current. Figure 8 presents the measurement results made on the test vehicles. Voltage swing at the output of the readout circuit is strongly increasing with the variations. An increase up to 45% can be reached at saturation level for variation process #3. However, an increase of dark current can be seen for this variation process. A trade off must be made because variation process #4 offers a improvement of the voltage swing at the output (33% of increase at saturation level) with a slightly increase of dark current.



a) Sensitivity curve for the standard process and the 4 implant variations

PROCESS	Linearity @5% (mV)	Saturation level (mV)
STANDARD	716	872
VARIATION #1	984	1115
VARIATION #2	1029	1166
VARIATION #3	1121	1266
VARIATION #4	1021	1163

	Dark Current @30°C in nA/cm²
Standard T	0,33
Var1	0,82
Var2	0,72
Var3	0,71
Var4	0,40

b) Measured voltage swing at the output of circuit and dark current density

Figure 8 : Sensitivity, voltage swing at the output of the readout circuit and dark current density measurement results

Using the result of the dynamic range equation for this readout circuit, a comparison of dynamic range in dB can be made between the different process (standard and variations) for an integration time of 100ms. Calculations are made

using the saturation level (ie  $V_{MAX}$ ) and the maximum voltage allowing a non-linearity inferior to 5%. Figure 9 shows the dynamic range with regard to the process variation and for  $\alpha=1$  and  $\alpha=2$ .

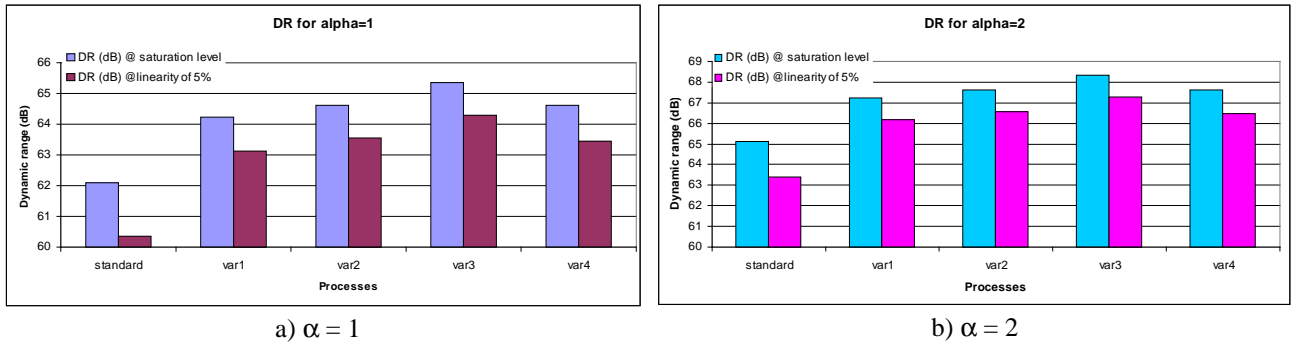


Figure 9 : Dynamic range in dB

A real improvement of the dynamic range can be reached, up to 4 dB for the process variation #3. A trade off between DR and dark current can be made and process variation #4 is the more efficient in this case. Indeed, an increase of 3.5dB is obtained without a significant degradation of dark current.

#### 4. READOUT CIRCUIT ARCHITECTURE IMPROVING DYNAMIC RANGE

Another way to improve dynamic range of CMOS image sensors is to modify readout architecture. The equation (1) shows the impact of reset noise on dynamic range. For a common 3T photodiode with a classical readout circuit (two stages, c.f. previously), the reset noise is dominant. If the reset noise is eliminated, the dynamic range increases and becomes, without neglecting the other noise terms :

$$DR = \frac{V_{MAX} - V_{DARK}}{\sqrt{V_{NOISE\_DARK}^2 + \frac{V_{READOUT\_NOISE}^2}{A_{TOT}^2}}}$$

A new readout circuit architecture can be implemented to eliminate reset noise. This architecture is composed of 3 sample and hold circuits allowing sampling of reference signal and photonic signal in the same frame as required for a CDS readout mode [8][9]. This architecture is suitable for linear or multi linear sensors. So, the DR becomes :

$$DR = \frac{V_{MAX} - V_{DARK}}{\sqrt{\sigma_{NOISE\_DARK}^2 + \sum \sigma_A^2 + \sum \sigma_{SH}^2}}$$

- $V_{MAX}$  = Maximum linear voltage on the photodiode (or readout node)
- $V_{DARK}$  = Voltage due to dark current
- $\sigma_{NOISE\_DARK}$  = Noise voltage due to dark current
- $\sigma_{RESET}$  = Noise voltage due to reset phase
- $\sum \sigma_A$  = Sum of noise voltage due to amplifier stages
- $\sum \sigma_{SH}$  = Sum of noise voltage due to S/H phases



Figure 10 : DEMOS vehicle photography

This architecture was implemented in a test vehicle named DEMOS. A photography of DEMOS is depicted in Figure 10. This test vehicle is a multi-linear sensor.

This multi-linear sensor is composed of lines with 7.5 $\mu\text{m}$  pixel pitch and lines with 15 $\mu\text{m}$  pixel pitch. Each line has a readout circuit dedicated with a CDS (Correlated Double Sampling) implemented. Pixel rate on the 2 video output is close to 3 MPix/s.

The UMC CIS 0.35 $\mu\text{m}$  process was used. Variation 3 for the photodiode doping implant was re-used for this test vehicle (cf previous section). Conversion gain of the 7.5 $\mu\text{m}$  pixel pitch is close to 7.8 $\mu\text{V/e}$ . Conversion gain of the 15 $\mu\text{m}$  pixel pitch is close to 3 $\mu\text{V/e}$ .

Measurements made on this vehicle allow to compute the Dynamic range value for this sensor. A comparison with the same sensor without CDS stage can be made when taking into account reset noise. This comparison is made with the

“hard reset mode”, i.e. reset noise is equal to  $\sqrt{\frac{kT}{C_{PH}}}$ . Results on dynamic range are presented in Figure 11 for the both pixel pitch. An output readout noise of 147 $\mu\text{V}$  was found in both cases.

An output swing voltage close to 840mV was measured for the readout circuit allowing a 1% maximum non-linearity. The output swing voltage was close to 1.06V at saturation level. A gain of 0.6 was measured for the readout circuit.

For comparison, the reset noise was carried out with photodiode capacitance close to 12fF for 7.5 $\mu\text{m}$  pixel pitch and close to 32fF for 15 $\mu\text{m}$  pixel pitch.

Results show an increase of 8dB in terms of dynamic range for the small pixel and an increase of 6dB for 15  $\mu\text{m}$  pixel pitch.

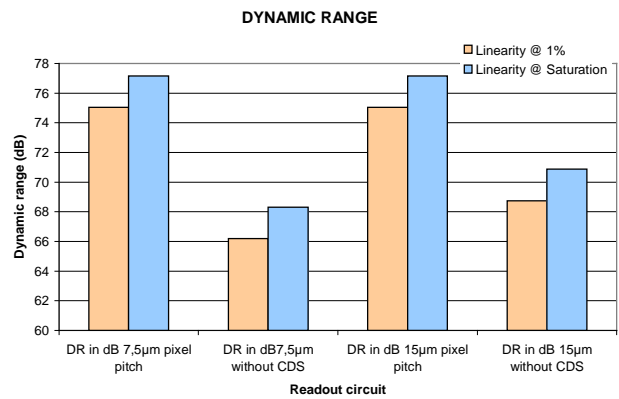


Figure 11 : Dynamic range comparison

As expected, the dynamic range increases when reset noise, the dominant noise, is eliminated. The dynamic range becomes independent of the photodiode size, i.e. the capacitance value. A real improvement of dynamic range is achieved by architecture design.

## 5. CONVERSION GAIN CONTROL IN ORDER TO IMPROVE DYNAMIC RANGE

Equation 1 in section 2 shows the relation between dynamic range (DR) and conversion gain ( $G_c$ ). Indeed, conversion gain, which is dependent of photodiode size through capacitance value, impacts the reset noise. If a readout chain without correlated double sampling (CDS) is used, the reset noise is not cancelled and is dominant compared to other noises (assuming a pixel size close to 13 $\mu\text{m}$  and 0.35 $\mu\text{m}$  lithography process). Nevertheless, for large photodiode capacitance, assumption concerning the reset noise predominance becomes false and all noise sources must be taken into account.

For the common 3T pixel 2D topology where CDS readout cannot be easily applied DR can be enhanced by decreasing the conversion gain. Indeed, conversion gain increasing, for a 3T pixel without reset noise cancellation device (CDS), the reset noise increases. If reset noise increases, with a fixed voltage output swing, the dynamic range decreases. In addition, the photodiode full well capacity decreases while conversion gain increases. Figure 12 depicts DR behavior function to Conversion gain variation.

$$DR = \frac{V_{MAX} - V_{DARK}}{\sqrt{V_{NOISE\_DARK}^2 + 2 \cdot \frac{kT}{\alpha q} G_{C\_PH} + \frac{V_{READOUT\_CIRCUIT}^2}{A_{TOT}^2}}}$$

With :  $V_{MAX}$  = Maximum linear voltage on the photodiode (or readout node)  
 $V_{DARK}$  = Voltage du to dark current  
 $V_{NOISE\_DARK}$  = Noise voltage du to dark current  
 $V_{READOUT\_CIRCUIT}$  = Noise voltage du to readout circuit  
 $\alpha$  : coefficient between 1 and 2 = hard reset ( $\alpha \approx 1$ ) and soft reset ( $\alpha \approx 2$ )  
 $G_{C\_PH}$  : Conversion gain on the integration node (or readout node)  
 $A_{TOT}$  = Readout circuit gain

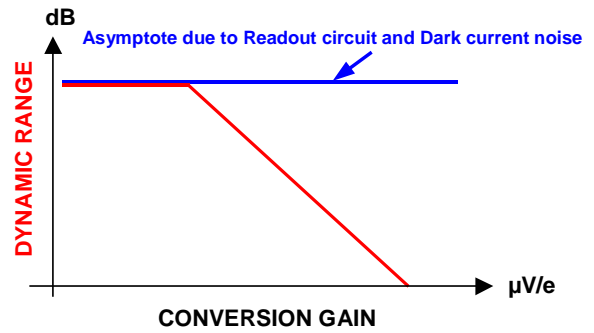
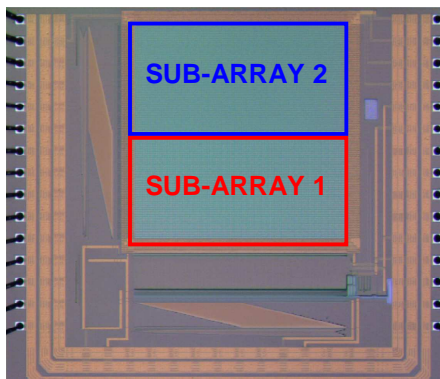
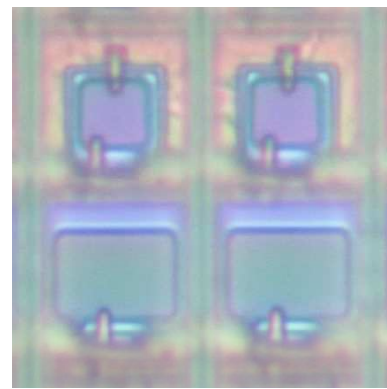


Figure 12 : Dynamic range versus Conversion gain

Test vehicles were designed to demonstrate control gain feasibility. These test vehicles are based on 128x128 pixel array (2D array) with two conversion gain variation by vehicles. Pixel pitch is 13μm. The readout circuit is composed of two stages as COBRA1M in section 3. Figure 13 shows a microphotography of one of the test vehicles.



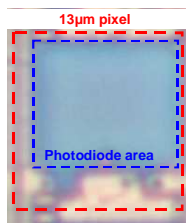
a) One of the test vehicles with 2 sub-arrays



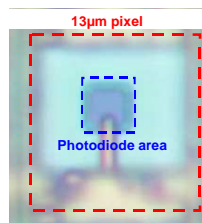
b) Example of pixels on test vehicles

Figure 13 : Microphotography of the test vehicle designed for Conversion Gain control

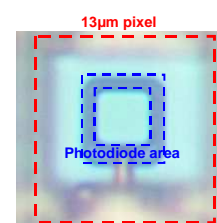
Various techniques for conversion gain control was achieved using different methods, depending on the final aim (i.e. an increase or a decrease of the conversion gain). The first technique consists in reducing the photodiode capacitance which allows to increase conversion gain. Figure 14 b) and c) presents two ways to do it.



a) Reference pixel



b) Photodiode area decrease type 1



c) Photodiode area decrease type 2

Figure 14 : Ways to increase conversion gain

This technique consists in decreasing the photodiode area in order to decrease its capacitance. Two ways are taken into account to reduce photodiode capacitance : Type 1 ( Figure 14 b) and Type 2 ( Figure 14 c).



The second technique consists in increasing the photodiode capacitance which allows to decrease conversion gain. Figure 15 presents two ways to do it.



a) Photodiode capacitance increase type 1

b) Photodiode capacitance increase type 2

Figure 15 : Ways to decrease conversion gain

This second technique consists in increasing capacitance of the photodiode by adding a fixed capacitance within pixel. A fill factor degradation is noted and will imply degradation on spectral detection efficiency (SDE).

Table 1 sum up variation of conversion gain designed. For comparison, a reference structure with a conversion gain of  $5.1 \mu\text{V/e}$  was also designed. This reference structure has a photodiode area as large as possible (STRUCTURE # 11).

Structure 1	26 $\mu\text{V/e}$	Reducing photodiode area (type 1)	Structure 6	1,4 $\mu\text{V/e}$	Increase photodiode capacitance (type 1)
Structure 2	21 $\mu\text{V/e}$	Reducing photodiode area (type 1)	Structure 7	1,1 $\mu\text{V/e}$	Increase photodiode capacitance (type 1)
Structure 3	13 $\mu\text{V/e}$	Reducing photodiode area (type 2)	Structure 8	0,7 $\mu\text{V/e}$	Increase photodiode capacitance (type 2)
Structure 4	9,4 $\mu\text{V/e}$	Reducing photodiode area (type 2)	Structure 9	0,4 $\mu\text{V/e}$	Increase photodiode capacitance (type 2)
Structure 5	1,8 $\mu\text{V/e}$	Increase photodiode capacitance (type 1)	Structure 10	0,3 $\mu\text{V/e}$	Increase photodiode capacitance (type 2)

TABLE 1 : Conversion gain variation tested

Figure 16 depicts measurement results on conversion gain value.

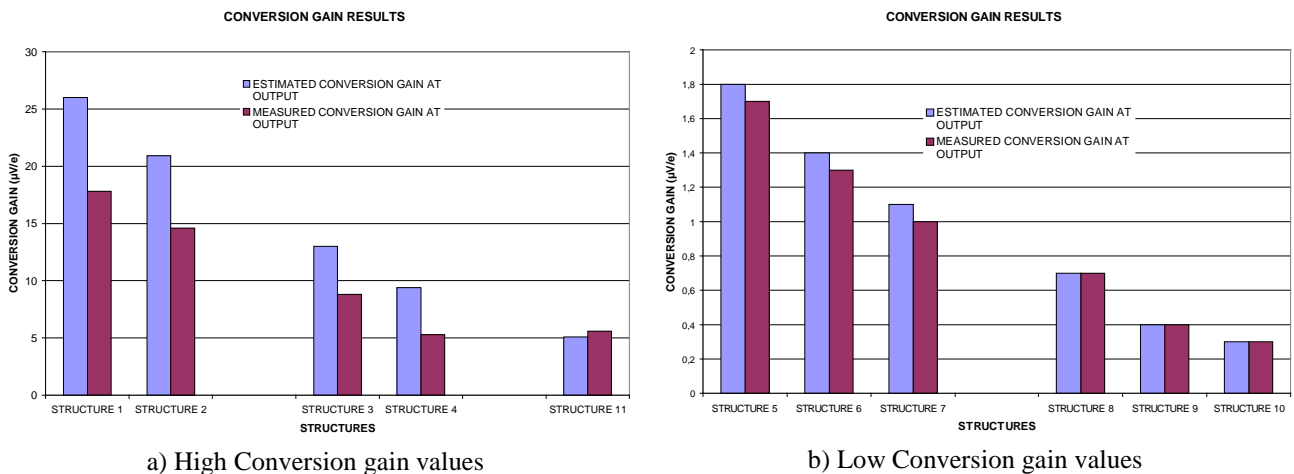


Figure 16 : Conversion gain measurement results

As expected, conversion gain measurement results show conversion gain variation between structures. A good control on it is achieved for low conversion gain. However, a difference can be noted for high conversion gain. This difference is

explained by process difficulties to control with accuracy some doping implants. It is also explained by difficulties to estimate photodiode capacitance. Indeed, only surface capacitance was taken into account for photodiode capacitance estimation (no perimeter capacitance was taken into account). A control of the conversion gain is demonstrated with variation in the range of 0.05 to 3 of initial conversion gain.

Noise and linearity measurements allows to calculate dynamic range. Figure 17 shows the dynamic range for these different structures.

Dynamic Range measurement results show a improvement of dynamic range for low conversion gain structures, as expected. Dynamic range beyond 75dB can be reached. This increase of dynamic range in this case implies to a spectral detection efficiency degradation.

A control of dynamic range is achieved using these techniques through the conversion gain control which determine reset noise level.

Further measurements will be made to evaluate crosstalk and FTM response.

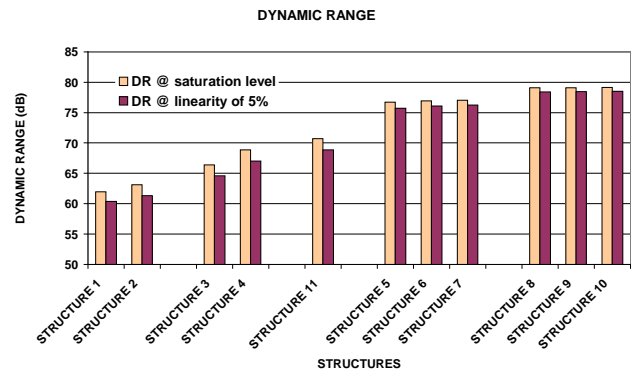


Figure 17 : Dynamic range measurement results

## 5. CONCLUSION

Different techniques for dynamic range improvement were investigated and reported in this paper. Several test vehicles were designed by CIMI in collaboration with EADS-Astrium to perform comparison between theoretical values and measurements. The first technique oriented on process improvement gives very good results with a dynamic range increase close to 3.5dB with only a slightly increase of dark current (a dynamic range improvement close to 4 dB can be obtained but a dark current degradation is expected). The second technique which is based on improvement of readout circuit architecture allowing a real CDS readout gives also good results. In this case, an increase of 8 or 6 dB (depending of the photodiode size) can be achieved. Readout circuit size is enlarged to allow correlated double sampling. The third technique consists to control conversion gain. Ways to control conversion gain (in the range of 0.05 to 3) were presented and measurements results show a control on dynamic range. Further measurements will be made to refine results on crosstalk and FTM for these techniques.

## ACKNOWLEDGMENTS

The authors want to thank Paola Cervantes and Celine Engel (Supaero Integrated Image Sensors Laboratory) for numerous test vehicles characterizations. The authors are grateful to EADS-Astrium for financial support.

## REFERENCES

1. M. Furumiya and al, « High sensitivity and No-Crosstalk pixel technology for embedded CMOS Image Sensor », IEEE TRANSACTIONS ON ELECTRON DEVICES, Vol. 48, NO. 10, October 2001.
2. H. Ihara and al, « A 3.7 x 3.7  $\mu\text{m}^2$  square pixel CMOS image sensor for digital still camera application », in ISSCC Tech. Dig., Feb. 1998, pp. 182-183.
3. O.-B. Kwon and al, « An improved digital CMOS imager », in Proc. IEEE Workshop Charge-Coupled Devices and Advanced Image Sensors, June 1999, pp. 144-147.
4. Bedabrata Pain, Thomas J. Cunningham, and Bruce Hancock, «Noise Sources and Noise Suppression in CMOS Imagers, Focal Plane Arrays for Space Telescopes », Jet Propulsion Laboratory, California Institute of Technology,

edited by Thomas J. Grycewicz, Craig R. McCreight, Proceedings of SPIE Vol. 5167 (SPIE, Bellingham, WA, 2004)

5. Hui Tian, Boyd Fowler, and Abbas El GamaI, «Analysis of Temporal Noise in CMOS Photodiode Active Pixel Sensor », IEEE JOURNAL OF SOLID-STATE CIRCUITS, VOL. 36, NO. 1, JANUARY 2001
6. B. Fowler and al, «Reset noise reduction in capacitive sensors», IEEE Transactions on Circuits and Systems, Vol.53, N°8, Aug. 2006.
7. Pierre Magnan, « Detection of visible photons in CCD and CMOS:A comparative view », Nuclear Instruments and Methods in Physics Research A 504 (2003) 199–212.
8. Degerli and al, « A Fast monolithic Active Pixel Sensor with pixel -Level Reset noisesuppression and Binary outputs for charge particles detection », IEEE Transactions On Nuclear Science, VOL. 52, NO. 6, december 2005
9. Lepage and al, « CMOS long linear array for space application », Sensors, Cameras, and Systems for Scientific / Industrial Applications VII., Proceedings of the SPIE, Volume 6068, pp. 61-68 (2006).